JOURNAL OF Applied Polymer SCIENCE

Curing Behavior of Epoxy Resins in Two-Stage Curing Process by Non-Isothermal Differential Scanning Calorimetry Kinetics Method

He Sun,[1,2] Yuyan Liu,[1,2] Youshan Wang,[2] Huifeng Tan[2]

[1]School of Chemical Engineering and Technology, Harbin Institute of Technology, Harbin 15000, China

[2]National Key Laboratory of Science and Technology on Advanced Composites in Special Environments, Harbin Institute of Technology, Harbin 150001, China

Correspondence to: Y. Liu (E-mail: liuyy@hit.edu.cn) and Y. Wang (E-mail: wangys@hit.edu.cn)

ABSTRACT: In this research, a new thermal curing system, with two-stage curing characteristics, has been designed. And the reaction behaviors of two different curing processes have been systematically studied. The non-isothermal differential scanning calorimetry (DSC) test is used to discuss the curing reaction of two stages curing, and the data obtained from the curves are used to calculate the kinetic parameters. Kissinger-Akahira-Sunose (KAS) method is applied to determine activation energy (E_a) and investigate it as the change of conversion (α). Málek method is used to unravel the curing reaction mechanism. The results indicate that the curing behaviors of two different curing stages can be implemented successfully, and curing behavior is accorded with Šesták-Berggren mode. The non-isothermal DSC and Fourier transform infrared spectroscopy test results reveal that two different curing stages can be implemented successfully. Furthermore, the double x fitting method is used to determine the pre-exponential factor (A), reaction order (m, n), and establish the kinetic equation. The fitting results between experiment curves and simulative curves prove that the kinetic equation can commendably describe the two different curing reaction processes. © 2014 Wiley Periodicals, Inc. J. Appl. Polym. Sci. **2014**, *131*, 40711.

KEYWORDS: differential scanning calorimetry (DSC); kinetics; resins

Received 11 November 2013; accepted 13 March 2014

DOI: 10.1002/app.40711

INTRODUCTION

Epoxy resin, a kind of the most important thermosetting polymer, is used as composite materials, structural adhesives, surface coatings, and electronic encapsulating materials widely, due to its chemical resistance, adhesion, good electrical properties, simple process ability, and lower cost.[1–3] Most of the commercially available epoxy resin is diglycidyl ether of bisphenol-A (DGEBA).[4] But, in some cases, the mechanical property and heat resistance of epoxy resin cannot meet certain requirements, which are the disadvantages to limit its application. To settle the question, some researchers add various particles into matrix resin or blend epoxy resin with other polymers to improve their properties.[5–7] In this study, we propose a different method to improve the mechanical property and heat resistance of epoxy resin, two-stage curing method. Furthermore, the curing process has been studied. The base to propose this method is shape memory function of epoxy resin system as our previous research.[8,9]

The two-stage curing system contain matrix epoxy resin E51, room temperature curing agent 593 and latent curing agent 594, and these two curing agents have rarely reciprocity between each other. Herein, E51 is the acronym of matrix epoxy resin, 593 and 594 are the acronyms of room temperature curing agent and latent curing agent, respectively. The two-stage curing method include two different curing stages, for the first-curing stage, the curing reaction takes place between E51 and 593, and 594 does not participate in the reaction by controlling the curing condition. For the second-curing stage, 594 was triggered to react with remainder unreacted matrix resin by raising environment temperature. This method is different from conventional multistep curing or post curing.[10–12] The two-stage curing process can be described as following and drawn in Figure 1.

1. Room temperature curing agent and latent curing agent were added into epoxy resin matrix synchronously (E51:593 and E51:594 both have 100% theoretical conversion), and stirring uniformly. Then, the mixtures were dumped into mould of presetting shape.
2. First-stage curing was triggered at room temperature, and the polymers formed materials I with the desired shape. During this curing period, the latent curing agent would not be triggered by controlling the curing conditions.

© 2014 Wiley Periodicals, Inc.

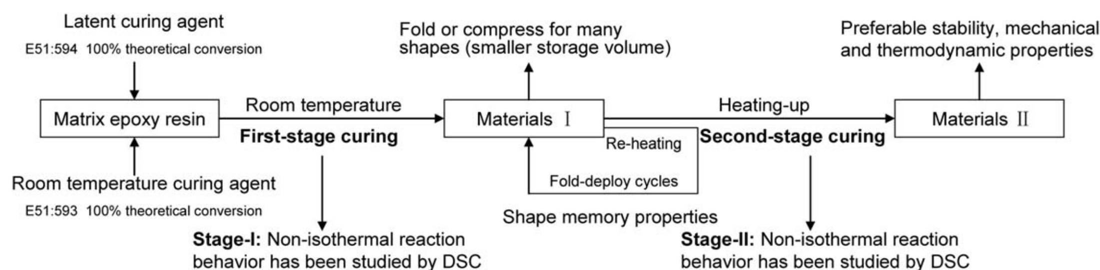

Figure 1. The two-stage curing process.

3. If the presetting shape of material was too big to storage or transportation expediently, Materials I could be folded to different size (tube or rectangle shape) by heating to make it soft. That shape memory effect is the innovation point of two-stage curing method.
4. The folded components of materials I can recovery to their original shape by heating temperature to above glass transition temperature (T_g), which indicates that materials I can be fold-deploy repeatedly. It is useful and convenient for materials to test in different conditions.
5. If the components need to be used, raising temperature to trigger second stage curing, then materials II can be formed. The heat resistance and mechanical strength of materials would be improved after second-stage curing.

The main aim of this study was to investigate the reaction kinetics of two different curing stages. Herein, the curing reaction kinetics had been studied by the non-isothermal differential scanning calorimetry (DSC) technology. Málek method[6,13–15] and iso-conversional method of Kissinger-Akahira-Sunose (KAS)[16–18] were applied to unravel the curing reaction mechanism and activation energy (E_a) of two curing stages. The pre-exponential factor (A) and reaction order (m, n) were tried to obtain by double x fitting method.

EXPERIMENTAL

Materials

The polymer matrix used in this study was bisphenol A glycidyl ether epoxy resin E51, with epoxy value 0.5 ± 0.01 (epoxy equivalent weight 196–204 g eq^{-1}, and n in the chemical structure is 0.18–0.24) purchased from Bluestar Chemical New Materials Co. The room temperature curing agent was a modified amine, 593, it was a transparent liquid and had long-chain structures provided by Shanghai Resin Co., and the viscosity was 80–100 mPa s (298.15 K). The latent curing agent was β, β'-dimethylamino ethoxy-1,3,6,2-dioxin boron (594) obtained from Huayue Viscose Chemical Co. All materials were used without further purification. The chemical structures of reactants were shown in Figure 2. It could be observed from the structures of two different curing agents, the reactive activity between them was unlikely.

Curing Schedule

For our previous researches, the fact that two different curing stages almost not influence each other had been confirmed.[19] The preparation process and curing schedule were done as follows:

1. Curing agents 593 and 594 were added into epoxy resin matrix synchronously, then stirred the mixtures for 3 min. After that, the mixtures were placed for about 5 min until it became almost transparent and no bubbles.
2. For the first-curing stage, that was E-51/593 system, the mixtures were cured at room temperature for 24 h, followed by curing in air oven at 353.15 K for 2 h, and then allowed to cool slowly to room temperature. Material I had been prepared. Using this curing schedule, the second-curing stage was not triggered in our previous researches.[19]

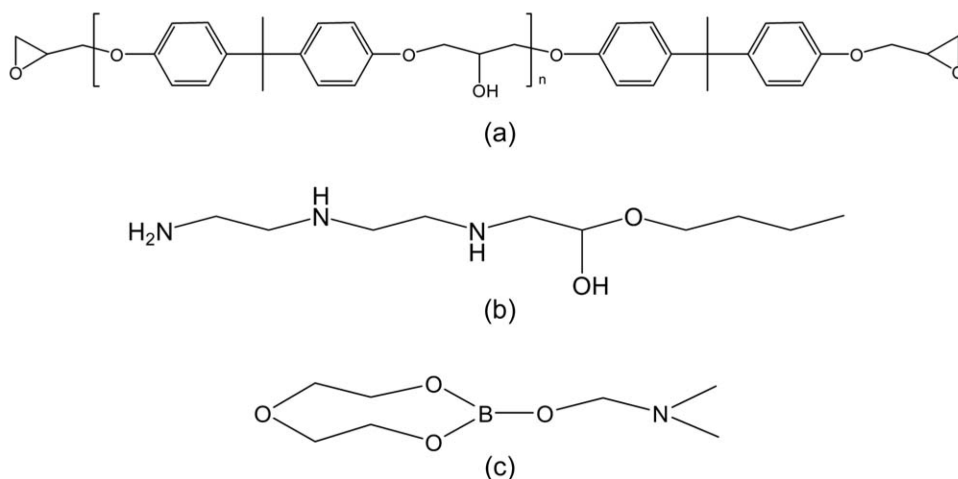

Figure 2. Chemical structures of epoxy resin and curing agent.

3. For the second-curing stage, that was E-51/594 system, material I was performed at 403.15 K for 2 h, and curing at 443.15 K for 3 h, followed again by slow cooling to room temperature, then material II had been prepared. Furthermore, there was almost no epoxy groups existed in material II, obtained from Fourier transform infrared spectroscopy (FTIR) test results.

DSC Measurements

Study on the curing kinetics of E51/593 and E51/594 systems were performed by DSC. The non-isothermal DSC measurements were performed with Mettler Toledo Instruments for data acquisition, it was calibrated with high purity indium, and experiments were conducted under a nitrogen flow of 20 cm^3 min^{-1}. In DSC experiments, the samples (3–4 mg) were added to aluminum pans and analyzed dynamically with heating rates at 5, 10, 15, and 20 K min^{-1}.

As the E51/593/594 system had two relatively independent curing stages, the DSC test was divided into two stages:

1. The E-51/593/594 mixtures tested in 5, 10, 15, and 20 K min^{-1} from 293.15 to 410.15, 420.15, 430.15, and 440.15 K, respectively. Then, we suspended the test and allowed the sample cool slowly.
2. The specimens stayed for 2 h at room temperature.
3. The systems were re-heated from 293.15 to 653.15 K in 5, 10, 15, and 20 K min^{-1}.

The reason for using this test method was that the test process of non-isothermal DSC was a continuous heating mode, which was different from the practical curing schedules describing in Curing Schedule section. Hence, if using the continuous heating mode, environment would provide heat to system continuously, and might lead to a greater reaction heat gathered in the mixtures. This reaction heat could not dissipate fast enough, so the second stage curing step would be triggered in advance. Thus, using the two stages DSC test method could avoid this problem effectively.

RESULTS AND DISCUSSION

Basic Assumptions of Curing Kinetics

There are a few approaches to analyze the curing kinetics by DSC[20–26] test. In this study, the non-isothermal experiment is used to investigate the curing kinetics of E51/593/594 system. In general, there are three basic assumptions for the application of DSC to the curing of polymers.

Assumption one: The area between the base line and the curve over a period of a certain time is proportional to the total area, and the ratio can be defined as conversion (α):[6]

$$\alpha=\frac{\int_0^t H dt}{H_T}=\frac{\int_0^t H dt}{H_E+H_R} \tag{1}$$

where H is the DSC heat flow (kJ mol^{-1}), H_T is the entire heat released when an uncured material is completely cured, H_E is the heat enthalpy by the first heating scan, H_R is the residue heat enthalpy by the second heating scan, $H_T = H_E + H_R$, and t is reaction time (s).

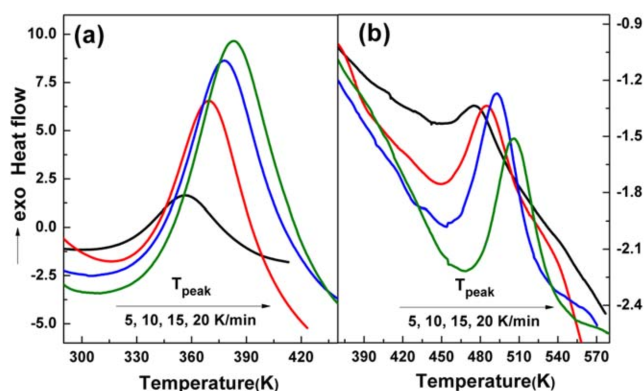

Figure 3. Non-isothermal heat flow curves for the reaction of first stage curing (a: E51/593) and second stage curing process (b: E51/594). [Color figure can be viewed in the online issue, which is available at wileyonlinelibrary.com.]

Assumption two: The rate of the kinetic process is proportional to the measured heat flow:

$$\frac{d\alpha}{dt}=\frac{dH/dt}{H_T} \tag{2}$$

where $d\alpha/dt$ is reaction rate, and dH/dt is the partial heat of reaction at time t.

Assumption three: The basic reaction rate equation for dynamics analysis can be expressed as follows:

$$\frac{d\alpha}{dt}=k(T)f(\alpha) \tag{3}$$

where $k(T)$ is reaction rate constant, $f(\alpha)$ is mathematical expression of curing kinetics model, and T is absolute temperature (K). $k(T)$ is conform to the Arrhenius formula, showed in eq. (4):

$$k(T)=A\exp\left(-\frac{E_a}{RT}\right) \tag{4}$$

where A is the pre-exponential factor, E_a is the activation energy (kJ mol^{-1}), R is the gas constant [8.314 J (mol K)$^{-1}$].

Non-Isothermal Curing Reactions Curves

The non-isothermal DSC test curves for the reaction of E51 with 593 and E51 with 594 at different heating rates are presented in Figure 3, and the baselines of each curves are adjusted by analysis software STAR^e. Figure 3(a) exhibits the enthalpy curves of first stage curing (E51/593), while Figure 3(b) presents the second stage curing process (E51/594). It can be seen that the peak temperature rises with the increasing of heating rate. Because the samples have temperature hysteresis effect during non-isothermal DSC test, in other words, the heating rate is faster, the temperature of samples need to achieve the uniform conversion is higher. The DSC curing peak characteristics for stage-I and stage-II are listed in comparison in Table I.

From Table I, it can be seen that $T_{\text{pre-peak}}$ (stage-II) is higher than $T_{\text{past-peak}}$ (stage-I) at the same heating rate between two different curing stages, which indicates that the second curing stage has not been triggered before the first curing stage completes. The data of DSC curing peak characteristics prove that the two different curing stages can be implemented successfully, and the effect between the two step curing is rare, they can occur independently.

Table I. The DSC Curing Peak Characteristics for Stage-I and Stage-II

Curing stage	Heating rate (K min^{-1})	Non-isothermal DSC curing peak characteristics			
		$T_{pre\text{-}peak}$ (K)	T_{peak} (K)	$T_{past\text{-}peak}$ (K)	$H_T = H_E$ (kJ mol^{-1})
Stage-I	5	303.86	358.98	411.22	204.42
	10	310.19	369.69	420.69	239.87
	15	315.99	377.30	438.21	277.36
	20	317.77	382.96	445.51	256.94
Stage-II	5	435.22	474.23	506.67	64.65
	10	447.40	486.58	526.29	55.23
	15	449.83	492.59	541.06	55.20
	20	467.51	505.81	577.04	50.92

$T_{pre\text{-}peak}$ and $T_{past\text{-}peak}$ are the initial and final integration temperatures, respectively.

As previously stated, $H_T = H_E + H_R$, Figure 3(b) shows that there is no exothermic peak from 350 to 450 K, indicating H_R (stage-I) = 0, so H_T (stage-I) = H_E (stage-I). To calculate H_T (stage-II), the mixtures of materials II re-heat from 293.15 to 653.15 K in 5, 10, 15, and 20 K min^{-1}, the result shows that there is no exothermic peak also, hence, H_T (stage-II) = H_E (stage-II). The data list in Table I. For the two independent curing processes, conversion (α) can reach 100% for the first curing stage (E51/593), and α of second curing stage can also get to 100% (E51/594). The non-isothermal curves of α versus T for the reaction in stage-I and stage-II plot in Figure 4. Y-axis includes α-I and α-II of two curing stages. Figure 4 exhibits that 435 K is critical point between stage-I and stage-II curing process. That is the first stage curing has been completed before 435 K, and the second stage curing starts from 435 K, hence, the two curing stage almost have no influence each other.

FTIR Analysis

FTIR test is used to detect the epoxy group absorption peaks in different composites, and the FTIR spectra curves of pure E51, after stage-I curing process and after stage-II curing process systems are shown in Figure 5(a). The peak appears from 3440 to 3400 cm^{-1} is the characteristic absorption peak of —OH. The peaks observe from 3000 to 2860 cm^{-1} are caused by stretching vibration of C—H. The absorption bands at 1606, 1508, and 1458 cm^{-1} are attributed to C=C stretching vibration on aromatic ring. Compare pure E51 curve with after stage-I and stage-II curing process curves, the absorption peaks from 1104 to 1077 cm^{-1} have been appeared, which are the characteristic absorbance peak of ether C—O—C, the results prove that curing agent 593 has reacted with matrix resin. The peak at 831 cm^{-1} is the characteristic absorption peak of benzene ring. In general, the characteristic absorption peak of epoxy group is 930–908 cm^{-1}, hence, the wavenumber from 1000 to 700 cm^{-1} has been magnified in Figure 5(b). In the curve of pure E51 system, the characteristic absorption peak of epoxy group in 913 cm^{-1} can be observed obviously. After stage-I curing process, the characteristic absorption peak of epoxy group can still be traced, but the area of absorption peak reduces significantly, indicating that the epoxy groups react with curing agent. After stage-II curing process, the characteristic absorption peak of epoxy group is hardly noticeable, presenting that remaining epoxy groups have

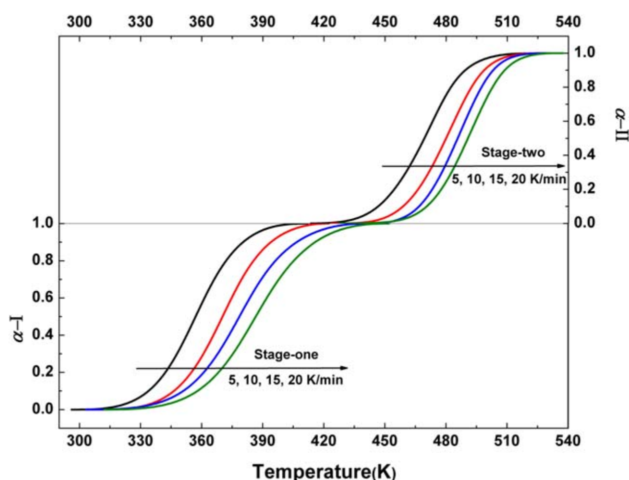

Figure 4. Non-isothermal curves α-I and α-II versus T for the reaction of stage-I and stage-II. [Color figure can be viewed in the online issue, which is available at wileyonlinelibrary.com.]

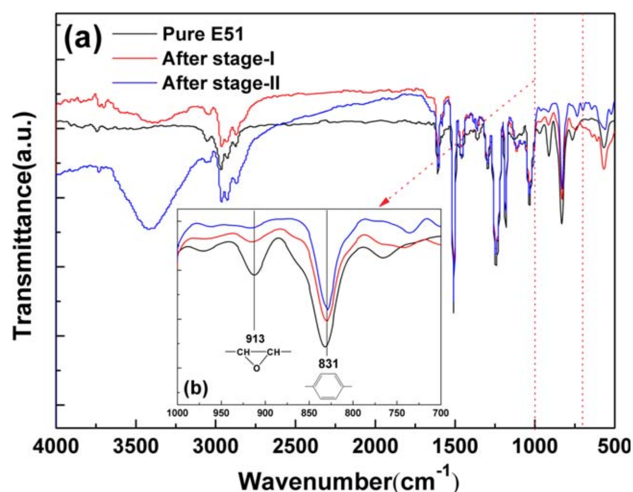

Figure 5. The FTIR test results of pure E51, after stage-I curing process and after stage-II curing process systems. [Color figure can be viewed in the online issue, which is available at wileyonlinelibrary.com.]

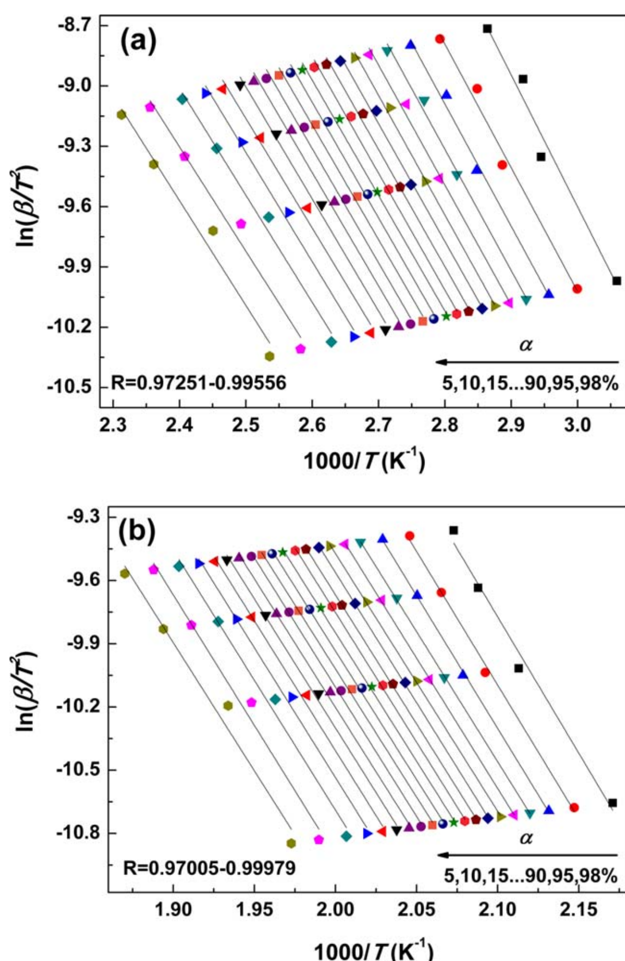

Figure 6. Iso-conversional KAS lines for the (a) E51 with 593 and (b) E51with 594. [Color figure can be viewed in the online issue, which is available at wileyonlinelibrary.com.]

reacted with the latent curing agent. Furthermore, the second curing has been triggered, and the reaction is complete.

The FTIR test results reveal that two different curing stages can be successfully implemented, and the latent curing agent reacts with the remainder of the epoxy resin completely.

Model-Fitting Kinetics

Málek proposed a complete thermal analysis method for most probable mechanism function in kinetic study. In this article, it is used to analyze the non-isothermal kinetic. For this method, it needs to get E_a. The integral iso-conversional KAS method is used to determine E_a and investigate it as the change of conversion.

KAS equation of the final form is derived as follows:[27]

$$\frac{\ln \beta}{T^2} = -\frac{-E_a}{RT} + \ln\left(\frac{AR}{E_a}\right) - \ln g(\alpha) \quad (5)$$

$$g(\alpha) = \int_0^{\alpha} \frac{d\alpha}{f(\alpha)} \quad (6)$$

where β is heating rate (5, 10, 15, and 20 K min^{-1} in this research), $g(\alpha)$ is conversion function showing in eq. (6). Figure 6 shows the plots of $\ln(\beta/T^2)$ versus $1/T$ for E51/593(stage-I) and E51/594(stage-II). Herein, $\alpha = 5, 10, 15\ldots 90, 95$, and 98%. E_a can be solved from the every slope of a linear plot of $\ln(\beta/T^2)$ versus $1/T$. It can be seen that the straight line fitting rate is good, $R = 0.97251$–0.99556. Data of activation energy draw in Figure 7, and the error bars mark in the graphs. In general, the errors of DSC test come from temperature fluctuate, baseline drift, non-uniform sampling, linear or nonlinear curve fit, and different heating rate. From the data of this study, it can be seen that the error is less than 5%, and R is more than 97%, so we think the results are reliable.

As shown in Figure 7, there is a reduction trend of E_a-stage-I (from 55.484 to 49.482 kJ mol^{-1}) with conversion increases (5%–30%). This phenomenon can be explained as follows: in the initial of curing reaction, the mixture viscosity decrease as the increasing temperature.[28] The low viscosity leads to better mixing which is conductive to reaction, hence, E_a-stage-I decreases. When the conversion exceeds 30%, the E_a-stage-I is stabilized at the constant value (about 48.5 kJ mol^{-1}). It might be caused by the increased molecular weight, which further leads to enhanced viscosity, reaction temperature and conversion, these factors have both positive and negative effects to the energetic barriers.[29] When the conversion exceeds 90%, the crosslink density of mixtures increase and the reactive groups decrease, leading the curing reaction become more difficult, so the E_a increased. For the E_a-stage-II, it can be observed that E_a does not vary with α significantly, because the second curing stage is triggered in viscoelastic state environment, the viscosity change is very small. By calculating, the mean of E_a is 48.534 ± 2.731 kJ mol^{-1} for stage-I, and 102.550 ± 2.848 kJ mol^{-1} for stage-II.

For Málek method, once E_a is determined, two characteristic functions, $y(\alpha)$ and $z(\alpha)$ can be defined to find the kinetic model. In non-isothermal conditions, the two functions can be described as follows:

$$y(\alpha) = \beta\left(\frac{d\alpha}{dt}\right)\exp(x) \quad (7)$$

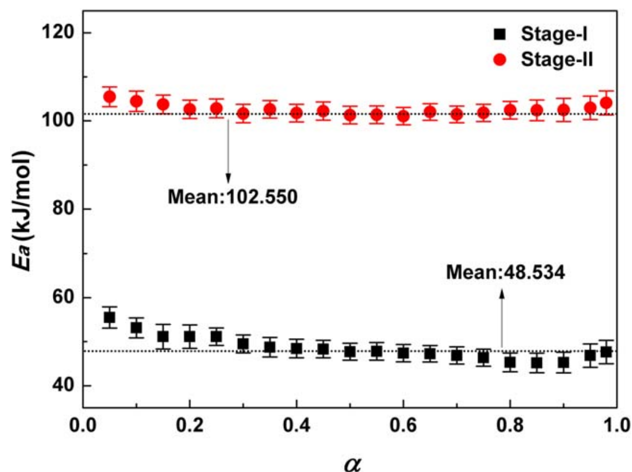

Figure 7. Plots of activation energy (E_a) as function of conversion for stage-I and stage-II. [Color figure can be viewed in the online issue, which is available at wileyonlinelibrary.com.]

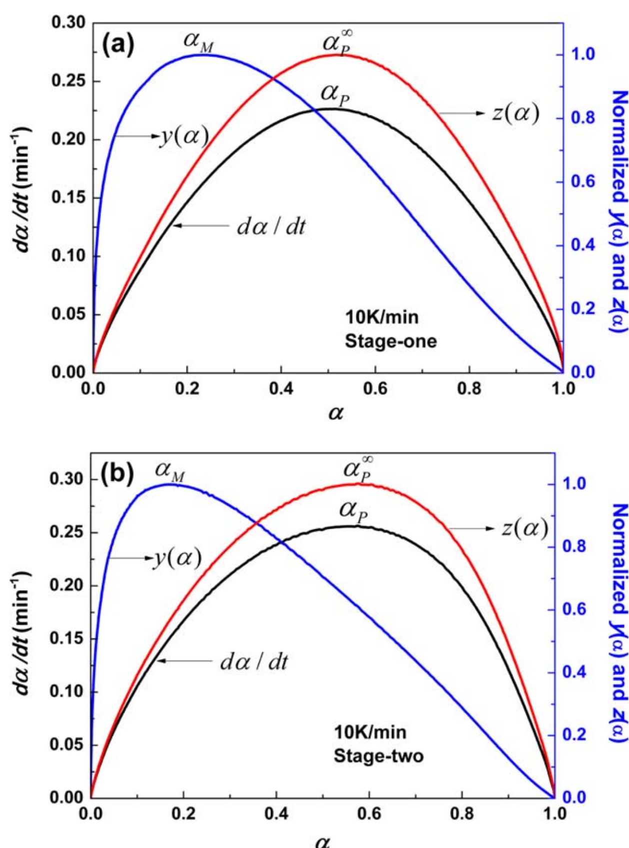

Figure 8. Variation of experimental reaction rate ($d\alpha/dt$), normalized $y(\alpha)$ and $z(\alpha)$ versus fractional conversion for (a) stage-I and (b) stage-II curing with the heating rate of 10 K min^{-1}. [Color figure can be viewed in the online issue, which is available at wileyonlinelibrary.com.]

$$z(\alpha)=T\left(\frac{d\alpha}{dt}\right)\pi(x) \tag{8}$$

$$x=\frac{E_a}{RT} \tag{9}$$

where $\pi(x)$ is the function of temperature integral whose values can be approximated with sufficient accuracy with a fourth-order rational expression of Senum and Yang:[14,20–33]

$$\pi(x)=\frac{x^3+18x^2+88x+96}{x^4+20x^3+120x^2+240x+120} \tag{10}$$

After a series of calculation, the variation of experimental reaction rate ($d\alpha/dt$), normalized $y(\alpha)$ and $z(\alpha)$ versus fractional conversion for stage-I and stage-II curing process are presented in Figure 8, the curve obtains from 10 K min^{-1} heating rate as an example. The peak values of $d\alpha/dt$, $y(\alpha)$, and $z(\alpha)$ are indicated α_M, α_P and α_p^∞, respectively. The detailed results are listed in Table II.

From Table II, it can be seen that α_M=0.231, 0.232, 0.240, 0.238, α_p^∞=0.528, 0.530, 0.538, 0.532 for stage-I, α_M=0.162, 0.169, 0.173, 0.170, α_p^∞=0.599, 0.603, 0.610, 0.623, respectively, for stage-II, so $0<\alpha_M<\alpha_p^\infty$, and $\alpha_p^\infty \neq 0.632$. Based on dynamics model choice plotted by Málek[14] and the shape of $y(\alpha)$ and $z(\alpha)$, we may conclude that the Šesták-Berggren model is suitable to fit the non-isothermal reaction rates of stage-I and stage-II curing process, and the model is widely used in literatures[34–36] for epoxy systems. The Šesták-Berggren model can be expressed as follows:

$$\frac{d\alpha}{dt}=A\exp\left(-\frac{E_a}{RT}\right)\alpha^m(1-\alpha)^n \tag{11}$$

where m is the order of autocatalytic reaction, n is the order of reaction with curing agent, and the other parameters have the same meaning as equations listed before.

We substitute mean E_a 48.534 kJ mol^{-1} (stage-I) and 102.550 kJ mol^{-1} (stage-II) respectively into eq. (11). Because every T and α correspond to a same $d\alpha/dt$, the double x fitting method is used to determine the A, m, and n. The fitting results list in Table III.

Table III presents that the fitting rate is well, $R \geq 0.99$. Based on the mean of A, m, and n, the kinetic equation can be established for stage-I and stage-II. Then, every T and α of different heating rate are substituted into kinetic equation of stage-I and stage-II severally, which is obtained from the average values of the parameters. Then experimental curves at four different heating rate can been drawn. The comparison between experimental curves and simulation curves reveal in Figure 9.

In Figure 9, the full lines are experiment data curves, it can be observed that there are two relatively independent peaks except the heating rate of 20 K min^{-1} curve. There is a small discontinuous area between the two curing stage in 20 K min^{-1} curve. It can be explained that the DSC test have temperature hysteresis effect for the chemical reaction, the faster heating rate makes the curing reaction to need higher temperature. Hence, we may draw a conclusion that fast heating rate is an unfavorable condition for two-stage curing. The suitable heating rate of non-isothermal DSC test is less than 10 K min^{-1}. The dotted lines are simulation curves, it can be seen that dotted lines are very similar with full lines, which proves that the kinetic equation

Table II. Characteristic Peak Conversion Values, α_M, α_P, and α_p^∞ for Stage-I and Stage-II with Heating Rates of 5, 10, 15, and 20 K min^{-1}

	Stage-I			Stage-II		
β (K min^{-1})	α_M	α_P	α_p^∞	α_M	α_P	α_p^∞
5	0.231	0.508	0.528	0.162	0.563	0.599
10	0.232	0.515	0.530	0.169	0.573	0.603
15	0.240	0.519	0.538	0.173	0.580	0.610
20	0.238	0.510	0.532	0.170	0.574	0.623

Table III. Calculated Kinetic Parameters A, m, and n of Šesták-Berggren Model for Stage-I and Stage-II

Stage	β (K min^{-1})	A	m	n	Adj. R-Square
Stage-I	5	7.9057×10^{10}	0.24196	1.2641	0.99762
	10	8.7631×10^{10}	0.26837	1.1582	0.99907
	15	1.0343×10^{11}	0.29599	1.1111	0.99907
	20	1.0729×10^{11}	0.33135	1.1362	0.99906
	Mean	9.4352×10^{10}	0.28442	1.1674	—
	Kinetic equation	$\frac{d\alpha}{dt}=9.4352\times10^{10}\cdot\exp(-48534/RT)\cdot\alpha^{0.28442}(1-\alpha)^{1.1674}\alpha\in(0,1)$			
Stage-II	5	3.4254×10^{6}	0.33395	1.2889	0.99749
	10	3.7295×10^{6}	0.35438	1.2565	0.99682
	15	3.7041×10^{6}	0.33982	1.3613	0.99566
	20	3.2268×10^{6}	0.30164	1.3187	0.99906
	Mean	3.5215×10^{6}	0.33245	1.3064	-
	Kinetic equation	$\frac{d\alpha}{dt}=3.5215\times10^{6}\cdot\exp(-102550/RT)\cdot\alpha^{0.33245}(1-\alpha)^{1.3064}\alpha\in(0,1)$			

can describe the curing reaction process commendably, including stage-I and stage-II.

In general, the effect of kinetic equation is to guide the curing process. From the equation, it can be seen there are three variables, including α, T, and t. If two variables are provided with the actual operation needs, the third variable can be calculated basing on the kinetic equation. For example, conversion α has been given as 90% for stage-I, it can use two different methods to achieve this curing process, using longer time and lower temperature or using shorter time and higher temperature. So, the actual operation is more convenient and flexible. On the other hand, the different conversion corresponds to different glass transition temperature (T_g). Because of the crosslink density of curing system decreases with the conversion reduces, and in general, T_g is proportional to the crosslink density. Such as front say, materials I possesses shape memory properties, it can be folded to different size (tube or rectangle shape) by heating to make it soft, for our previous study,[19] its T_g is suitable for softening. Thus, a certain T_g of study system is given, α will be determined, then, the appropriate T and t can be selected to prepare materials I.

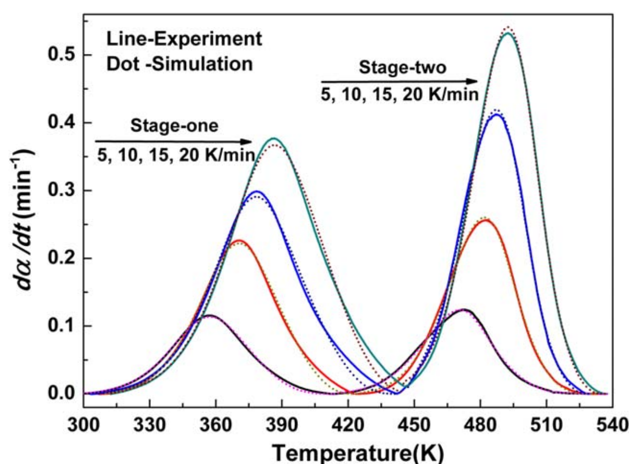

Figure 9. Comparison between experimental curves and simulation curves. [Color figure can be viewed in the online issue, which is available at wileyonlinelibrary.com.]

Overall, the credible kinetic equation can guide the reactive process well and make the actual operation has flexibility. It is of great significance to the application of materials.

CONCLUSION

The curing reaction behaviors of E51 with 593 and E51 with 594 had been systematically studied by non-isothermal DSC technique. The DSC and FTIR results showed that the two different curing stages could be implemented successfully, and the effect between the two stages curing was rare. The model-fitting reaction kinetic analysis with the Málek method proved the typical autocatalytic characteristic. The activation energy was calculated by KAS method, 48.534 ± 2.731 kJ mol^{-1} for stage-I and 102.550 ± 2.848 kJ mol^{-1} for stage-II, respectively. The further research confirmed that the Šesták-Berggren model was satisfactorily suitable for kinetic prediction of both two curing stages. Moreover, the double x fitting method was used to determine the kinetic parameters (A, m, and n), and the kinetic equation-stage-I and kinetic equation-stage-II had been established. Compared with experiment and fitting curves, it could be reached a conclusion that the kinetic equation could describe the curing reaction process well. This credible kinetic equation could guide the curing process well and make the actual operation more convenient and flexible.

ACKNOWLEDGMENTS

This work was financially supported by the Program for Harbin City Science and Technology Innovation Talents of Special Fund Project (2012RFXXG091) and Pre-research Fund Project of National Defense (9140C490105120C49187).

REFERENCES

1. Detwiler, A. T.; Lesser, A. J. *J. Mater. Sci.* **2012**, *47*, 3493.
2. Xie, T.; Rousseau, I. A. *Polymer* **2009**, *50*, 1852.

3. Pascault, J. P.; Williams, R. J. J. Epoxy Polymers: New Materials and Innovations, **2010**.
4. Roşu, D.; Caşcaval, C. N.; Mustată, F.; Ciobanu, C. *Thermochim. Acta* **2002**, *383*, 119.
5. Li, Y.; Xiao, F.; Wong, C. P. *J. Polym. Sci. Part A: Polym. Chem.* **2007**, *45*, 181.
6. Zhang, J.; Dong, H. X.; Tong, L. L. *Thermochim. Acta* **2012**, *549*, 63.
7. Ghaffaria, M.; Ehsania, M.; Khonakdar, H. A. *Thermochim. Acta* **2012**, *533*, 10.
8. Liu, Y. Y.; Sun, H.; Tan, H. F.; Du, X. W. *J. Appl. Polym. Sci.* **2013**, *127*, 3152.
9. Liu, Y. Y.; Han, C. M.; Tan, H. F.; Du, X. W. *Mater. Sci. Eng. A* **2010**, *527*, 2510.
10. El-ghayoury, A.; Hofmeier, H. *Macromolecules* **2003**, *36*, 3955.
11. Jiang, W.; Ding, Y. *Microelectron Eng.* **2008**, *85*, 458.
12. Bagis, Y. H.; Rueggeberg, F. A. *Dent. Mater.* **2000**, *16*, 244.
13. Yao, D.; Kuila, T.; Sun, K. B. *J. Appl. Polym. Sci.* **2012**, *124*, 2325.
14. Málek, J. *Thermochim. Acta* **1992**, *200*, 257.
15. Montserrat, S.; Andrew, G.; Cortes, P. *J. Appl. Polym. Sci.* **1996**, *61*, 1663.
16. Zvetkov, V. L.; Djoumaliisky, S.; Simeonova-Ivanova, E. *Thermochim. Acta* **2013**, *553*, 16.
17. Kissinger, H. E. *Anal. Chem.* **1957**, *29*, 1702.
18. Akahira, T.; Sunose, T. *Chiba Inst. Technol., Sci. Technol.* **1971**, *16*, 22.
19. Sun, H.; Liu, Y. Y.; Tan, H. F.; Du, X. W. *J. Appl. Polym. Sci.* **2014**, *131*, DOI: 10.1002/App.39882.
20. Wen, X. F.; Wang, W.; Cai, Z. Q. *Polym.-Plast. Technol.* **2011**, *50*, 1515.
21. Vyazovkin, S. *J. Comput. Chem.* **2001**, *22*, 178.
22. Vyazovkin, S.; Sbirrazzuoli, N. *Macromol. Rapid Commun.* **2006**, *27*, 1515.
23. Bao, Y. Q.; Gawne, D. T.; Zhang, T. *Surf. Coat. Technol.* **2012**, *207*, 89.
24. Garschke, C.; Parlevliet, P. P.; Weimer, C.; Fox, B. L. *Polym. Test.* **2013**, *32*, 150.
25. Ferdosian, F.; Ebrahimi, M.; Jannesari, A. *Thermochim. Acta* **2013**, *568*, 67.
26. Okabe, T.; Takehara, T.; Inose, K.; Hirano, N.; Nishikawa, M. *Polymer* **2013**, *54*, 4660.
27. Kandelbauer, A.; Wuzella, G.; Mahendran, A. *Chem. Eng. J.* **2009**, *152*, 556.
28. Sbirrazzuoli, N.; Vyazovkin, S.; Mititelu, A.; Sladic, C.; Vincent, L. *Chem. Phys.* **2003**, *204*, 1815.
29. Li, C.; Zuo, C. M.; Fan, H. *Thermochim. Acta* **2012**, *545*, 75.
30. Ramis, X.; Cadenato, A.; Salla, J. M.; Morancho, J. M.; Valles, A.; Contat, L.; Ribes, A. *Polym. Degrad. Stab.* **2004**, *86*, 483.
31. Zhang, G. P.; Cheng, J.; Shi, L. *Thermochim. Acta* **2012**, *538*, 36.
32. Roşu, D.; Mustată, F.; Caşcaval, C. N. *Thermochim. Acta* **2001**, *370*, 105.
33. Roşu, D.; Mititelu, A.; Caşcaval, C. N. *Polym. Test.* **2004**, *23*, 209.
34. Šesták, J.; Berggren, G. *Thermochim. Acta* **1971**, *3*, 1.
35. Šimon, P. *Thermochim. Acta* **2011**, *520*, 156.
36. Málek, J. *Thermochim. Acta* **1989**, *138*, 337.